



# HYBRID SIMULATION IN COMBINATION WITH HIGHLY COMPLEX AND NON-LINEAR NUMERICAL MODELS FOR SEISMIC PROTECTION OF ANTIQUE COLUMN STRUCTURES

F. Obón Santacana<sup>(1)</sup>, U. E. Dorka<sup>(2)</sup>, L. Petti<sup>(3)</sup>

<sup>(1)</sup> Research Engineer, University of Kassel, ferran.obon@uni-kassel.de

<sup>(2)</sup> Professor, University of Kassel, uwe.dorka@uni-kassel.de

<sup>(3)</sup> Professor, University of Salerno, petti@unisa.it

## Abstract

Hybrid simulation is a novel technique in which a numerical model is connected online with an experimental specimen, also called substructure, in the laboratory. So far the complexity of the models used has been limited small scale models coupled with not more than a couple of substructures either numerical or experimental, simultaneously.

The use of the *Subfeed* algorithm, an advanced hybrid simulation scheme that has been applied in a wide variety of applications not only in the civil engineering field but also in aerospace, allows increasing the size of the numerical models to a couple of thousands degrees of freedom even for real-time applications due to its parallel capabilities and exact treatment of experimental and numerical substructures. The key success of this algorithm is that it does not require any numerical model in order to predict the behaviour of the experimental specimen and proceed with the time integration.

This paper presents a study on the behaviour of this hybrid simulation algorithm when used together with a highly non-linear specimen, a 1:3 scale column replica of the temple of Neptune in Paestum (World Heritage Site) at the laboratory of the University of Kassel (Germany), and a complex and highly non-linear model of the temple. The 36 columns in the perimeter of the temple are modelled as a soft “engineer model” that will serve as a backbone. A node, with 6-Degrees of Freedom (DOF), will be placed at the centre of mass of each stone drum, echinus, abacus and architrave. This results, considering an average of 6 drums per column, in approximately 2000 DOFs. Between each of these DOFs, a three-dimensional non-linear constitutive law that describes the mechanics between stone blocks is placed and treated as a numerical substructure.

**Keywords:** Hybrid simulation; Subfeed algorithm; Tendon systems; Large numerical models; Seismic protection of antique column structures.

## 1. Introduction

Seismic protection of historical cultural heritage is an important aspect to consider if we want to keep these structures for the future generations. There have been attempts in the past to retrofit these structures, but the methods used were often too intrusive (reinforced concrete) and worsened in several cases the seismic performance of the building due to increased local stiffness that forbid the structure to behave in its natural way. Seismic retrofitting techniques offer more promising solutions for earthquake protection of these structures but they have not been validated for historical structures. Especially suitable is the tendon system, which is based on controlled motion of the rigid body mechanism. In it, tendons are installed inside the structure and the forces that develop in them during an earthquake have a stabilizing effect on the building, keeping the forces small and under control. It is in addition a system that can be removed at any time and has no external visual impact, a request when retrofitting historical buildings, as seen in [1] where steel bars with SMA devices were installed in the four corners of the bell tower of the San Giorgio church in Trignano, Italy.

Hybrid simulation is the chosen technique to validate this technique taking as a reference building the Temple of Neptune in Paestum, Italy. In this kind of simulation, the deformations provided by numerical model are transferred to the specimen (a substructure), and then the resulting forces are fed back to the numerical model. This technique allows changing the “virtual” position of the experimental column within the numerical mode, with and without tendon, can be changed. Then it can be observed how close to reality the behaviour is and the necessary numerical adjustments can be made in order to obtain a better and more refined model.



Figure 1. The Temple of Neptune in Paestum, Italy. [2]

## 2. The Sub-step force feedback (*Subfeed*) algorithm

The Sub-step force feedback (*Subfeed*) algorithm is a hybrid simulation algorithm developed by Dorka [3-17]. This scheme does not rely on predicting the future state of an experimental substructure and afterwards correcting the error as opposed to predictor corrector methods [18-21]. Instead, it relies on measured values at certain time intervals to proceed with the integration process. The *Subfeed* algorithm has been successfully applied in a wide variety of situations; major milestones include the first continuous substructure tests involving stiff-ductile specimen (time scale factor of 10) [2], the first real-time substructure tests (RTST) in aerospace [10], the first RTST on distributed shaking tables [11, 12], real-time hybrid simulation tests using an irregular steel frame and a bi-directional non-linear TMD [13] and the first continuous transoceanic hybrid simulation tests using a non-linear specimen [16].

The core of the *Subfeed* algorithm is a time discretization of the dynamic equilibrium equation with the particularity of having external forces coming from substructures that can be either numerical and/or experimental. Thus, this equation can be rewritten as follows in order to accommodate these external forces:

$$\mathbf{M}\ddot{\mathbf{u}} + \mathbf{C}\dot{\mathbf{u}} + \mathbf{K}\mathbf{u} = \mathbf{f}^l + \mathbf{f}^{c,a} + \mathbf{f}^{c,e} \quad (1)$$

Where  $\mathbf{f}^l$  is the external input force and  $\mathbf{f}^{c,a}$  and  $\mathbf{f}^{c,e}$  the force vectors coming from analytic and experimental substructures respectively. Using a finite element discretization of the displacements in the time domain (three points in time) and a weighted residual approach, as explained in [9], one can obtain a general formulation for all major integration algorithms that use three points in time:

$$\mathbf{u}_{n+1} = [\mathbf{M} + \gamma\Delta t\mathbf{C} + \beta\Delta t^2\mathbf{K}]^{-1} \cdot \left\{ \begin{aligned} & \left[ 2\mathbf{M} - (1-2\gamma)\Delta t\mathbf{C} - \left(\frac{1}{2} - 2\beta + \gamma\right)\Delta t^2\mathbf{K} \right] \mathbf{u}_n \\ & - \left[ \mathbf{M} - (1-\gamma)\Delta t\mathbf{C} + \left(\frac{1}{2} + \beta - \gamma\right)\Delta t^2\mathbf{K} \right] \mathbf{u}_{n-1} \\ & + \beta\Delta t^2\mathbf{f}_{n+1}^* + \left(\frac{1}{2} - 2\beta + \gamma\right)\Delta t^2\mathbf{f}_n^* + \left(\frac{1}{2} + \beta - \gamma\right)\Delta t^2\mathbf{f}_{n-1}^* \end{aligned} \right\} \quad (2)$$

Where  $\mathbf{u}$  is the discretized displacement vector in the time domain at time  $n$  and  $\mathbf{f}^* = \mathbf{f}^l + \mathbf{f}^{c,a} + \mathbf{f}^{c,e} = \mathbf{f}^l + \mathbf{f}^c$  the force vector. It is worth pointing out that the formulation can be extended to four points in time and discretize instead either velocities or accelerations. Note as well that the force vector has to be discretized using the same shape functions in order to maintain consistency. Since the reaction of the experimental subsystem  $\mathbf{f}_{n+1}^{c,e}$  can only be obtained through measurement, the use of iteration methods will lead to high frequency oscillations during the test, causing it to become unstable. In order to deal with this problem, the *Subfeed* treats any implicit time integration algorithm as a linear control equation within each time step and it relies on measured data in order to obtain the response of the subsystem. Eq. (2) is thus rewritten as a linear control equation splitting the known and unknown terms at the beginning of each time step:

$$\mathbf{u}_{n+1} = \mathbf{u}_{n+1}^0 + \mathbf{G}(\mathbf{f}_{n+1}^{c,a} + \mathbf{f}_{n+1}^{c,e}) \quad (3.1)$$

$$\mathbf{u}_{n+1}^0 = [\mathbf{M} + \gamma\Delta t\mathbf{C} + \beta\Delta t^2\mathbf{K}]^{-1} \cdot \left\{ \begin{aligned} & \left[ 2\mathbf{M} - (1-2\gamma)\Delta t\mathbf{C} - \left(\frac{1}{2} - 2\beta + \gamma\right)\Delta t^2\mathbf{K} \right] \mathbf{u}_n \\ & - \left[ \mathbf{M} - (1-\gamma)\Delta t\mathbf{C} + \left(\frac{1}{2} + \beta - \gamma\right)\Delta t^2\mathbf{K} \right] \mathbf{u}_{n-1} \\ & + \beta\Delta t^2\mathbf{f}_{n+1}^l + \left(\frac{1}{2} - 2\beta + \gamma\right)\Delta t^2\mathbf{f}_n^l + \left(\frac{1}{2} + \beta - \gamma\right)\Delta t^2\mathbf{f}_{n-1}^l \end{aligned} \right\} \quad (3.2)$$

$$\mathbf{G} = \beta\Delta t^2 [\mathbf{M} + \gamma\Delta t\mathbf{C} + \beta\Delta t^2\mathbf{K}]^{-1} \quad (3.3)$$

Where  $\mathbf{u}_{n+1}^0$  is the initial displacement vector, updated at the beginning of each time step, and  $\mathbf{G}$  is the gain matrix. Note here the same treatment for simulated and experimental substructures. The displacements (or velocities or accelerations in velocity or acceleration formulations respectively) obtained in Eq. (3.2) are introduced to the specimen/numerical substructure in small increments as specified by the ramp function in Eq. (4). Forces are measured at exactly the end of each increment, or sub-step, in order to obtain the displacement in Eq. (3.1).

$$\mathbf{x}_{n+1} = \mathbf{x}_n \left( 1 - \frac{k}{k^{sub}} \right) + \mathbf{x}_{n+1} \left( \frac{k}{k^{sub}} \right) \quad (4)$$

Where  $k^{sub}$  is the total number of sub-steps and  $k$  denotes the current sub-step. In this way, for each sub-step  $k$ , the displacement of the subsystem is computed, applied, and then the measured or calculated restoring forces are given as an input to the algorithm. The number of sub-steps is an important factor for the accuracy of the simulation as shown in [17], but 4 sub-steps provides sufficient accuracy for civil engineering applications. At the end of each time step, the equilibrium error can be compensated for the next time step.

$$\mathbf{e}_{n+1} = \mathbf{f}_{n+1}^l + \mathbf{f}_{n+1}^{c,a} + \mathbf{f}_{n+1}^{c,e} - (\mathbf{M}\ddot{\mathbf{u}}_{n+1} + \mathbf{C}\dot{\mathbf{u}}_{n+1} + \mathbf{K}\mathbf{u}_{n+1}) \quad (5)$$

This may be necessary, because equilibrium error can cause positioning errors, measurement errors and the effect of having a limited number of sub-steps to approximate the solution. Although a regular PID compensation e.g. with  $P = 0.95$  and  $I = D = 0$  has proven to be sufficient [6, 17], more advanced techniques, like adaptive error compensators can be also applied [14].

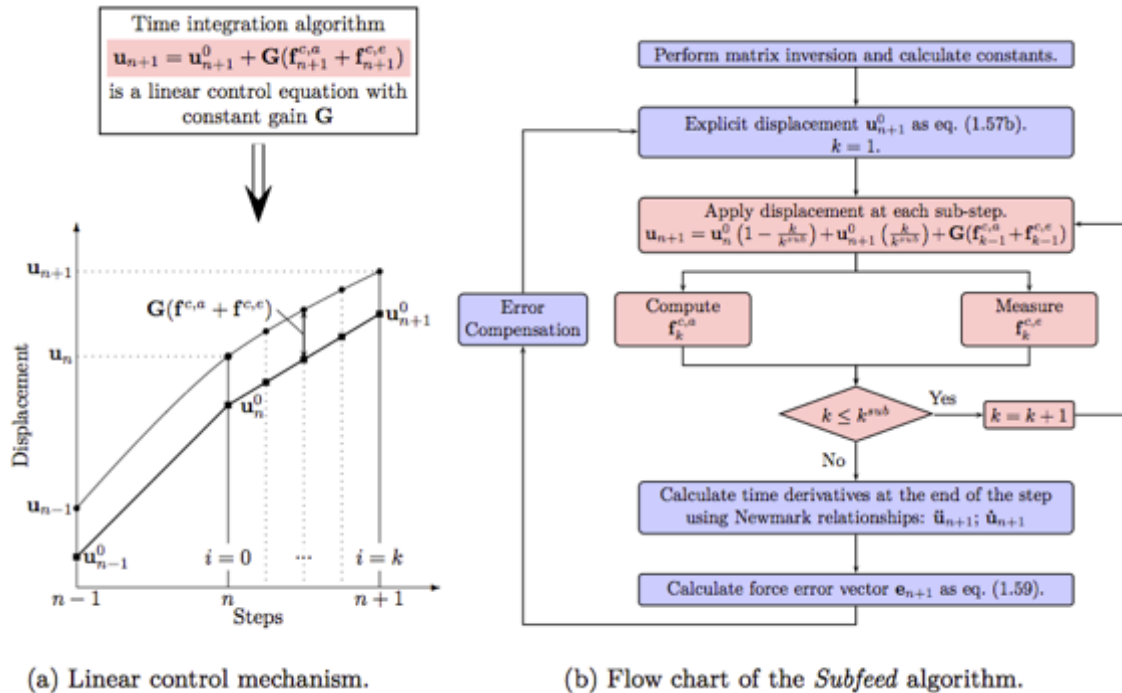


Fig. 2 – The Subfeed algorithm with the sub-stepping approach. Displacement control formulation.

### 3. Parallelisation and massive use of substructures

One of the objectives of this project is to obtain a numerical model of the mechanical behaviour of the stone drums using hybrid simulation. This requires having a large numerical model in order to accommodate all the drums in the columns present at the temple. The numerical model of the temple that is going to be used for the hybrid simulations is, therefore, of the order of 2000 dynamic degrees of freedom. Each on the drums, will have, in addition 3 dimensional numerical substructures applied, resulting in a total of 315 3D numerical subsystems and one experimental subsystem: the 1:3 scale column in the laboratory.

In order to execute each step of the *Subfeed* algorithm in a reasonable amount of time, a certain degree of parallelisation is required. On the linear algebra side, different possibilities have been given in the past [15] and where more thoroughly explored in [17]. Since the number of substructures is usually small and the vector of coupling forces has only non-zero elements where substructures are applied, one can efficiently reduce the amount of floating point in the inner loop (Fig. 2 red). This can be accomplished by dividing the degrees of freedom between those with substructures and those without. Only the degrees of freedom with coupling forces will partake in the operations in the inner loop. This results in the possibility of performing real-time hybrid simulation tests with numerical models of 2500 DOF with regular desktop computers [17].

In the current situation, nearly each degree of freedom has a coupling force applied, making the method described in the previous paragraph irrelevant. However, the *Subfeed* algorithm allows for the treatment of subsystems in parallel, meaning that task parallelisation on the substructure level is still possible. After all substructures are computed, the operation in Eq. (3.1) is performed and the process is repeated at every sub-step.

### 4. Numerical modelling

#### 4.1 Numerical model of the temple

In order to proceed with the time integration, the inverse of the term  $\mathbf{M} + \gamma \Delta t \mathbf{C} + \beta \Delta t^2 \mathbf{K}$  is required. This term, represents how much influence one degree of freedom has to another and is part of the  $\mathbf{G}$  matrix, requires matrices without zeroes in the diagonals. Since we want to have as less influence as possible on the non-linear actions described in the substructure, the Temple of Neptune is modelled featuring a soft backbone (Fig. 3) that connects all elements and thus, having all the diagonal terms of the stiffness matrix as non-zero. Each of the drums is a 6-DOF joint placed at the centre of mass instead of having it at the contact surface. Lumped masses are used. While the drums in the columns have non-linear behaviours attached, the stone blocks that form the entablature, architrave, frieze and cornice, do not since it is not possible to validate the numerical modelling with the current set-up. Instead, linear rotational springs are being used to connect the different elements in order to avoid complete separation. Further studies beyond the current project should focus on obtaining a validated numerical model of the system that forms the entablature. Only the outer perimeter of the temple is modelled.

In total, the numerical model consists of around 2100 DOF and has 315 three dimensional numerical non-linear substructures and one experimental substructure: the 1:3 scale stone column. Due to the advantages of hybrid simulation, the virtual position of experimental column will change between the following locations: side column, corner column and frontal column (Fig. 3).



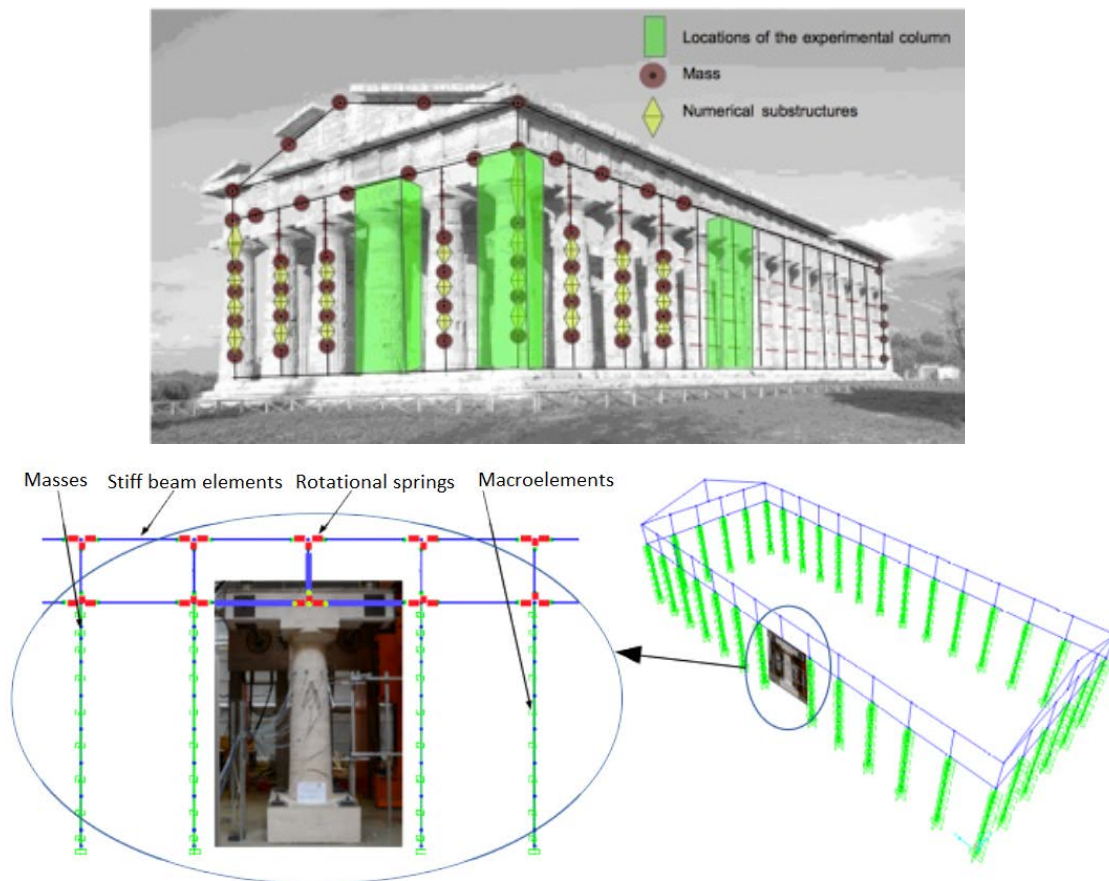


Figure 3. a) Sketch of the soft backbone of the temple model, with masses (red) at the centre of each drum and numerical substructures (yellow) connecting them. Locations of the experimental column in green. B) Numerical model of the temple.

#### 4.2 Modelling the mechanical behaviour of the stone drums

Each stone drum is connected to the upper and lower drum (when present) by three-dimensional non-linear macro elements that are treated as substructures. These non-linear elements are connected between the centres of mass of two consecutive drums since it is assumed that the central plane remains undeformed. As detailed in Fig. 4, symmetries in the mechanical behaviour of the stone drums will be exploited when defining the non-linear laws: sliding (in-plane translation), rotation against the vertical axis (torsion) and rotation against the two horizontal axis (rocking). It is assumed that two stone drums never lose contact. This leads to a 3-dimensional constitutive law in which the vertical normal force can be used as a surface parameter.

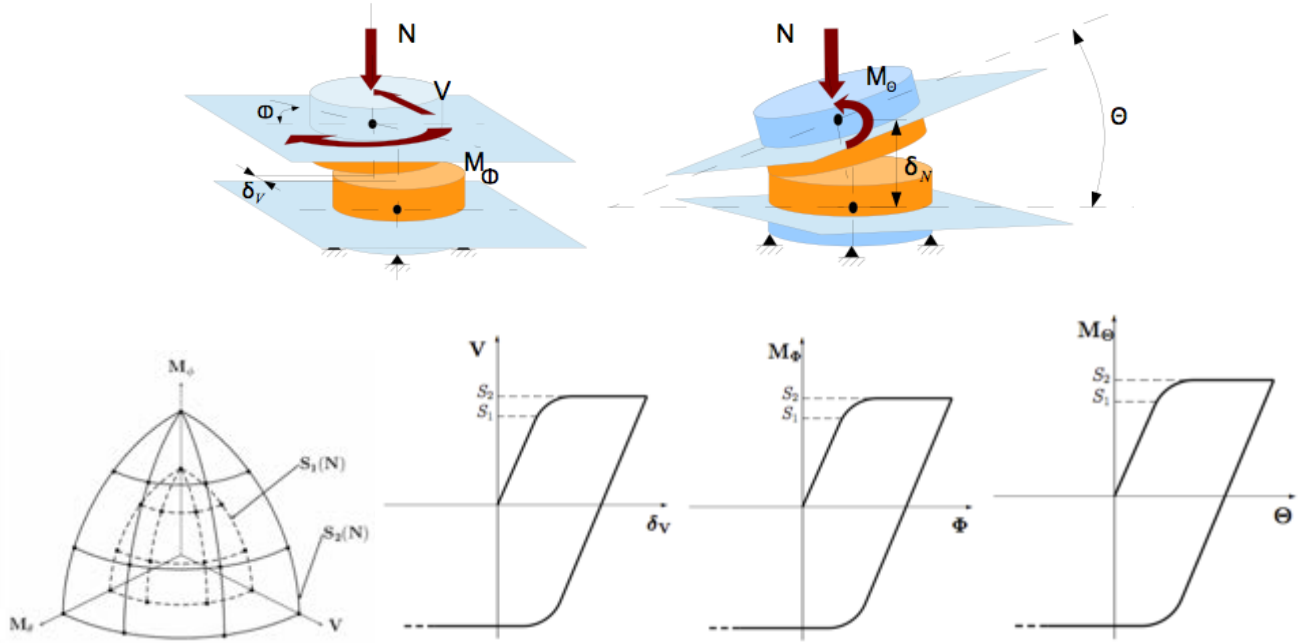


Figure 4 – By exploiting the symmetries of the experiments (top), 2-surface laws can be developed, which can be represented in 3-dimensions when the normal force  $N$  is used as a surface parameter (bottom left) as well as the a derivation of the surface ordinates from the non linear laws (bottom right).

This constitutive law is modelled as a numerical substructure in the *Subfeed* algorithm. The process of obtaining it requires, therefore, a transformation from the deformations from each node with 6-DOF (numerical model) to the local three-dimensional comprised of sliding  $\delta$ , torsion  $\Theta$ , and rocking  $\Phi$  (Eq. 6.1). The resulting restoring forces are transformed back (Eq. 6.2) and applied to the corresponding degree of freedom.

$$\begin{bmatrix} \delta \\ \Phi \\ \Theta \end{bmatrix} = \begin{bmatrix} \cos \alpha & \sin \alpha & 0 & 0 & 0 & 0 \\ 0 & 0 & 0 & \cos \beta & \sin \beta & 0 \\ 0 & 0 & 0 & 0 & 0 & 1 \end{bmatrix} \cdot \begin{bmatrix} u & v & w & \theta_x & \theta_y & \theta_z \end{bmatrix}^T \quad (6.1)$$

$$\begin{bmatrix} F_x \\ F_y \\ F_z \\ M_x \\ M_y \\ M_z \end{bmatrix} = \begin{bmatrix} \cos \alpha & 0 & 0 \\ \sin \alpha & 0 & 0 \\ 0 & 0 & 0 \\ 0 & \cos \beta & 0 \\ 0 & \sin \beta & 0 \\ 0 & 0 & 1 \end{bmatrix} \cdot \begin{bmatrix} F_\delta \\ F_\Phi \\ F_\Theta \end{bmatrix} \quad (6.2)$$

Where  $u$ ,  $v$  and  $w$  represent the displacement in  $x$ ,  $y$  and  $z$  directions,  $\alpha$  and  $\beta$  are the angles between the deformations in the  $x$  and  $y$  direction for deformations and rotations respectively, and  $F$  and  $M$  the restoring force and restoring moment respectively. Each state, sliding between drums, rocking and rotation are modelled using Bouc-Wen models [17] featuring both kinematic and isotropic hardening. Isotropic hardening, simulating the variation of normal force during an earthquake, is accomplished by changing the amplitude of the hysteresis loops through variation of the linear (yield) and limit (usually referenced as plastic) forces. The following formulation of the Bouc-Wen is used for modelling each of the components of the stone drum [22]:

$$\dot{z} = \frac{k_0}{f_l} \frac{\left\{ A\dot{u} - v \left[ \beta |\dot{u}| |z|^{n-1} z + \gamma \dot{u} |z|^n \right] \right\}}{\eta} \quad (7.1)$$

$$F = (1 - \alpha)k_0 u_{n+1} + \alpha F_y z \quad (7.2)$$

With  $A = A_0 - \delta_A \varepsilon$ ,  $v = 1 + \delta_v \varepsilon$ ,  $\eta = 1 - \delta_\eta \varepsilon$  and  $\varepsilon = (1 - \alpha)k_0 / f_l \dot{z}$  are the constitutive law deterioration parameters,  $\alpha$  the linear to non-linear stiffness ratio,  $\gamma$  and  $\beta$  shape variables,  $n$  defining the transition between linear and non-linear behaviour,  $k_0$  the elastic stiffness,  $f_l$  the linear force,  $z$  the hysteretic variable and  $F$  the resulting force for each state.

Although it may seem that at first glance each of the states are independent from each other, there is a non-linear constitutive relation for this macro-element when the surfaces start to move due to kinematic hardening. Once this kind of hardening occurs in any of the states, the surface in Fig. 4, changes position requiring an update of the linear and limit forces on the Bouc-Wen models that comprise the 3D substructure. Shape and degradation parameters should remain constant throughout the process. It must be emphasized that iterations in order to solve the non-linear differential equations of the Bouc-Wen models **do not** take place during the main loop (blue in Fig. 2). One can view instead, each of the 3D subsystems as separate and independent macro-elements in which a displacement is imposed and a restoring force is obtained as a result.

#### 4.2 Numerical comparison between the *Subfeed* algorithm and regular FE software

The soft back bone of numerical model of the temple used for the hybrid simulations was constructed using SAP2000. The resulting mass and stiffness matrices were exported and used in the parallel implementation of the *Subfeed* algorithm. Non-linear substructures (following the Bouc-Wen formulation found in SAP2000) were applied in the *Subfeed* algorithm while non-linear link elements of the type Bouc-Wen were defined in SAP2000. Since in this program it is not possible to define macro-constitutive laws, each of the non-linear substructures were independent from each other. The time history comparison between the solution offered by SAP2000 using non-linear direct time integration and Newmark ( $\beta = 0.25, \gamma = 0.5$ ) and the solution of the *Subfeed* using the same integration scheme, 4 sub-steps and having a PID as an error compensator with  $P = 0.95$  and  $I = D = 0$  can be seen in Fig. 5.

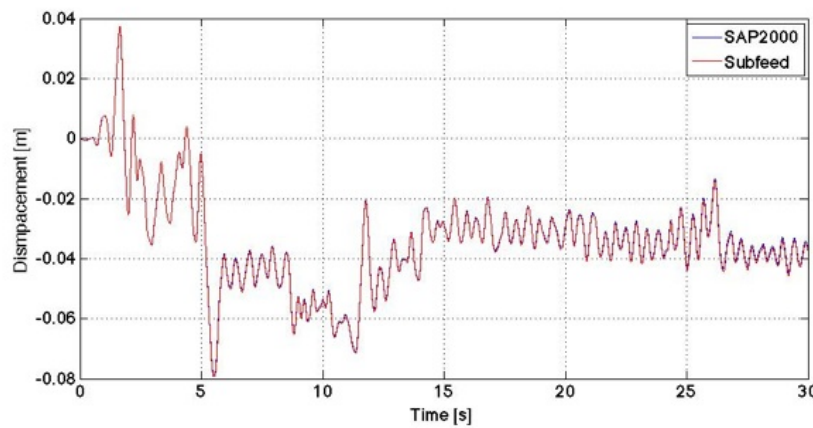


Figure 5 – Comparison between SAP2000 and the *Subfeed* algorithm. Using Newmark with  $\beta = 0.25, \gamma = 0.5$



## 5. Test set-up

The experimental column in the laboratory at the University of Kassel is a 1:3 scale replica of a column of the Temple of Neptune. The same type of stone, travertine, is used. The column consists of six drums on top of a base stone. Abacus, echinus and an architrave complete the set (Fig. 6). All the blocks have a hole in the middle that can accommodate the tendon system once it is active. The architrave serves as a loading introduction system, with 5 hydraulic cylinders connected to it. Each of the cylinders has a load capacity of 250 kN and can introduce motions up to  $\pm 200$  mm. Four of the cylinders are in displacement control, while the fifth (vertical cylinder on the right in Fig. 6) controls the total vertical force that is acting on the column through the motion of the two vertical cylinders. This normal force can be set either to be constant or to vary during the hybrid simulation test.

In order to measure the relative motion between two drums, a set of six high precision LVDTs, capable of measuring a displacement with a resolution of  $5\mu\text{m}$ , are installed between the central plane of each of the drums like a Steward platform [23]. The location of the Steward platform can be quickly changed between two consecutive tests in order to study different drums and obtain the necessary information required for identifying the 3D surface of Fig. 4.

A set of 32 strain gauges are embedded at the surface of the fifth drum starting from the bottom in order to measure the strains in the first 5 mm (see Fig. 6). The strain gauges can provide information on how the contact surface evolves during an earthquake and provide information regarding the strains that develop during the relative motion between two consecutive drums. This will be useful for the development of a detailed non-linear finite element model of to stone blocks.

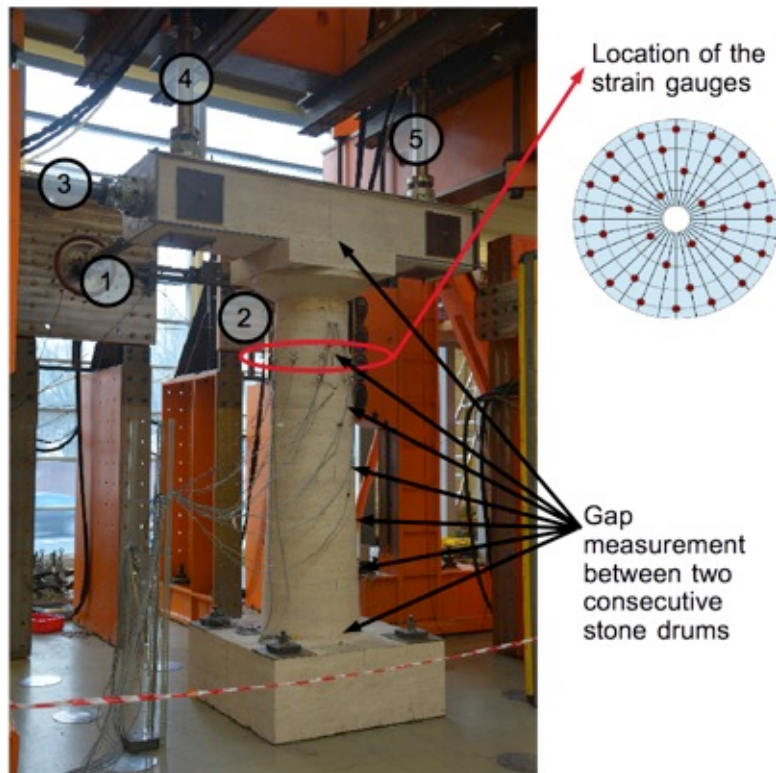


Figure 6 – Test set-up at the University Kassel featuring a 1:3 scale stone column replica with the cylinders 1 to 4 in displacement control and cylinder 5 controlling the vertical force of cylinders 4 and 5.

## 6. Hybrid simulation tests and numerical model update strategy

The hybrid simulation tests were conducted for the first time in April 2016. For these first experimental tests, the tendon system was not active and a constant normal force of 30 kN was applied. This level of force gives stresses similar to those present on the original columns which have only the architrave. The following testing program is envisaged in order to identify the drum mechanics, the behaviour of the tendon system and to refine the numerical model.

Table 1. Test plan. For each test, different column locations within the numerical model will be explored: Column on the long side with 58 kN additional vertical load, column on the corner with 58 kN additional vertical load and column on the short side with 98 kN vertical load.

|   | Tendon system  | Normal force level                  | Notes   |
|---|--|-------------------------------------|---|
| 1 | Not active   | Equivalent of 0.7g                  | Case 1: same earthquake record at 30 degrees.                 |
| 2 |  | Equivalent of 1g                    | Case 2: Independent earthquake records in x and y directions. |
| 3 |  | Equivalent of 1.3g                  |   |
| 4 |  | Variable due to vertical excitation | Three different earthquake records in x, y and z directions   |
| 4 | Active with springs of: 107.28, 149.1 and 189.9 N/mm | Equivalent of 0.7g                  | Case 1: same earthquake record at 30 degrees.                 |
| 5 |  | Equivalent of 1g                    | Case 2: Independent earthquake records in x and y directions. |
| 6 |  | Equivalent of 1.3g                  |   |
| 7 |  | Variable due to vertical excitation | Three different earthquake records in x, y and z directions   |

Fig. 7 (left) shows the hysteresis loops present at one of the horizontal cylinders, which introduces some rocking in the column, while Fig. 7 (right) shows the rocking motion between the upper drum and the one directly beneath it. With these experimental data (relative motion between the drums), the numerical model, especially the three-dimensional macro-constitutive relation, can be updated, which is underway at the time of writing. The process of updating will consist in comparing the measured hysteresis loops with the solution provided with the numerical solution given by the macro-constitutive relation. Shape and amplitude parameters of each Bouc-Wen model will be updated then accordingly. Once this iteration is performed, the position of the experimental column within the numerical model will be changed and the process will start again. The ultimate goal is to obtain a numerical model, through hybrid simulation, that can capture the behaviour of the experimental column.

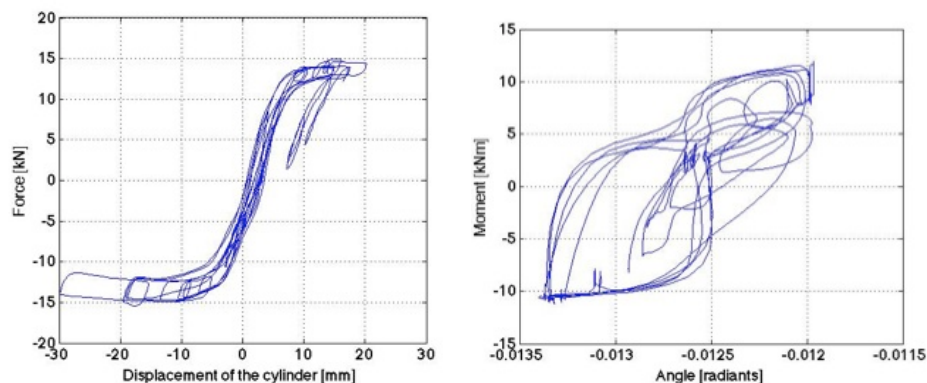


Figure 7 – Hysteresis loops measured at the architrave by the cylinder 3 (left) and relative rocking motion between the upper drum and the one directly beneath it (right).

## 7. Conclusions and future work

Hybrid simulation using a numerical model with around 2100 dynamic degrees of freedom and 315 non-linear three-dimensional substructures were performed using the *Subfeed* algorithm. The tests were performed continuously and with a time scale factor of 10. The numerical model was coupled on-line with a 1:3 scale stone column replica of the Temple of Neptune in Paestum, Italy. In order to introduce the different motions into the experimental column, 5 cylinders, 4 in displacement control and one in force control in order to keep the vertical force at a desired level, were used. It has been also demonstrated in this paper that the *Subfeed* algorithm provides the same results as using conventional FE software.

The project now is focusing in updating the three-dimensional constitutive relations that are used in order to model the mechanical behaviour of each stone drum. This is accomplished by direct comparison between experimental data, obtained by measuring the relative motion between two consecutive drums, and the results obtained by the numerical substructures.

The next step will consist on retrofitting the column with a tendon system: a 12mm diameter steel cable that is anchored at the base stone and has a spring at the top. The steel cable will not be pre-stressed and all the restoring forces will be caused by the compression of the spring. Since this spring should only provide the necessary force in order to take care of the P- $\Delta$  effect, a stiffness of 149.1 N/mm has been selected. Introducing a stiffer spring and/or pretension on the steel cable would only worsen the stabilizing effect of the tendon since although displacements will be reduced, forces acting on the overall system would increase. For the purpose of this project and in order to evaluate this effect, three springs are going to be evaluated in order to fully comprehend the effect they have on the tendon system, namely: 107.28, 149.1 and 189.9 N/mm.

## 8. Acknowledgements

The authors of this paper would like to thank the German Research Foundation (DFG) for the financial support of this project: Tendon Systems for Seismic Protection of Stone Block Historical Structures DO-360/25-1.

## 9. References

- [1] Castellano M. G., Indirli M., Martelli A., Azevedo J. J., Sincaian G. E., Tirelli D., Renda V., Croci G., Biritognolo M., Bonci A. Viskovic A. (1999): Seismic protection of cultural heritage using shape memory alloy devices – An EC funded project (ISTECH). *Proc. International Post-SMiRT Conference Seminar on Seismic Isolation, Passive Energy Dissipation and Active Control of Vibrations of Structures, I*, 417-443, Cheju, South Korea.
- [2] Image source. Web page: <http://www.paestum.org.uk>
- [3] Roik K., Dorka U. E. (1989): Fast online earthquake simulation of friction-damped systems. *Berichte / SFB 151*. Sonderforschungsbereich Tragwerksdynamic Ruhr-Universität Bochum, Germany.
- [4] Dorka U. E., Heiland D (1991): Fast online earthquake simulation using a novel PC supported measurement and control concept. *Structural dynamics: Recent advances*, 636-645, Elsevier Applied Science.
- [5] Dorka, U. E., Füllekrug U., Ji A., Gschwilm J. (1998): Algorithmen für real-time dynamische Substrukturtests. *Technical Report DFG 360/7-1*, Universität Kaiserslautern, Germany.
- [6] Bayer V., Dorka U. E. (2000): A New Algorithm for Real-Time Sub-Structure Pseudo-Dynamic Tests. *12<sup>th</sup> World Conference on Earthquake Engineering*, Auckland, New Zealand.

- [7] Bayer V., Dorka U. E. (2000): Qualification of TMDs by real-time SubPSD-testing. *2<sup>nd</sup> European Conference on Structural Control*.
- [8] Bayer V., Dorka U. E., Füllekrug U., Gschwilm J. (2002): Realisation of real-time pseudo-dynamic sub-structure. *International Conference on Noise and Vibration Engineering*.
- [9] Dorka U. E. (2002): Hybrid Experimental – numerical simulation of vibrating structures. *Proceedings of the Wave 2002 Workshop*, Yokohama, Japan.
- [10] Bayer V., Dorka U. E., Füllekrug U., Gschwilm J. (2005): On real-time pseudo dynamic sub-structure testing: algorithm, numerical and experimental results. *Aerospace Science and Technology*, **9**(3): 223-232.
- [11] Dorka, U.E., Queval J. C., Nguyen V. T., LeMaout A. (2006): Real-time sub-structure testing on distributed shaking tables in CEA Saclay. *4<sup>th</sup> World Conference on Structural Control and Monitoring*, San Diego, USA.
- [12] Dorka, U.E., Queval J. C., Nguyen V. T., LeMaout A. (2007): Substructure testing on distributed shake tables. *2<sup>nd</sup> International Conference on Advances in Structural Engineering*.
- [13] Khanlou N. M., Dorka U. E., Ristic D. (2011): Sub-structure testing on non-linear TMD using a hydraulic shake table. *4th International Conference on Earthquakes and Structures*, Seoul, South Korea.
- [14] Nguyen V. T., Dorka, U. E., Khanlou N. M. , Phan T.V. (2011): Real –time substructure tests of non-linear tuned mass damper using shaking table. *4th International Conference on Earthquakes and Structures*, Seoul, South Korea.
- [15] Obón Santacana F., Dorka U. E. (2012): Effects of large numerical models in continuous hybrid simulation. *15<sup>th</sup> World Conference on Earthquake Engineering*, Lisbon, Portugal.
- [16] Obón Santacana F., Dorka U. E. (2013): *Geographically distributed continuous hybrid simulation tests using shaking tables*. Proceedings of the Joint SERIES-NEES Workshop, JRC, Italy.
- [17] Obón Santacana F. (2015): Large numerical models in Continuous Hybrid Simulation. *Doctoral Thesis*. University of Kassel, Germany.
- [18] Nakashima N., Ishii K., Ando K (1990): Integration techniques for substructure pseudo-dynamic test. *Proceedings of the 4<sup>th</sup> International Conference on Earthquake Engineering*, **2**, 515-524.
- [19] Combescure D., Pegon P. (1997): Alpha-Operator splitting time integration technique for pseudo-dynamic testing error propagation analysis. *Soil Dynamics and Earthquake Engineering*, **16** (7-8), 427-443.
- [20] Chang S. Y. (2002): Explicit pseudodynamic algorithm with unconditional stability. *Journal of Engineering Mechanics*, **128** (9), 935-947.
- [21] Chen C., Ricles J.M. (2008). Development of Direct Integration Algorithms for Structural Dynamics using Discrete Control Theory, *Journal of Engineering Mechanics*, **134** (8), 676-683.
- [22] Baber T. T., Noori M. N (1985): Random vibration of degrading, pinching systems. *Journal of Engineering Mechanics*, **111** (8), 1010-1026.
- [23] Stewart D. (1966): A Patform with Six Degrees of Freedom. *Proceedings of the Institution for Mechanical Engineers (UK)*, **180** (Pt. 1, No. 15).

